The International Journal of Artificial Organs / Vol. 30 / no. 11, 2007 / pp. 000

Original article

A mathematical model comparing solute kinetics in low- and high-BMI hemodialysis patients

D. CRONIN-FINE[1], F. GOTCH[2,3], N. LEVIN[2], P. KOTANKO[2], M. LYSAGHT[1]

[1]Brown University, Providence, Rhode Island - USA
[2]Renal Research Institute, New York, New York - USA
[3]FMC-NA Research Laboratory, Walnut Creek, California - USA

ABSTRACT: Background: Patients with low Body Mass Index (BMI) on maintenance hemodialysis have a higher mortality risk than patients with elevated BMI. We investigated the use of kinetic modeling to test different hypotheses which have been advanced to explain this relationship. Methods: Equations from a three-pool urea-kinetic mathematical model (hepatic mass, extracellular fluid, muscle mass and adipose tissue) were solved to yield predictive profiles of solute and putative toxin concentrations versus time for patients of different body weights.
Results: For the interdialytic interval, our mathematic model suggests that extracellular solute/toxin concentration increases more rapidly in small patients. Additionally, time average concentration (TAC) is higher for this cohort. A lower value of the muscle mass and adipose tissue mass-transfer coefficient (K_{MMAT}), which determines the rate of solute release into the extracellular fluid, exacerbates this difference.
Conclusion: These results suggest that higher mortality for smaller dialysis patients may be mediated by higher time average toxin concentration, especially for solutes with a low mass-transfer coefficient value. (Int J Artif Organs 2007; 30:)

KEY WORDS: Kinetic modeling, Intercompartmental mass transfer, Dialysis mortality, BMI

INTRODUCTION

It is well established that physically smaller patients on maintenance hemodialysis carry a significantly higher mortality risk in comparison with larger patients (1-2). This finding is paradoxical because larger patients are at a much higher risk for cardiovascular disease and diabetes and thus, should have a higher mortality than smaller patients (3). However, this is not the case.

Two different explanations for this anomaly have been proposed. First, the high metabolic rate compartment (HMRC), i.e. visceral organs, which produces uremic toxins, is larger in proportion to the patient's body mass in small patients than in large patients. In other words, as a person increases in size, the ratio of HMRC to total body size decreases. As a consequence, small patients produce a larger quantity of toxins relative to their body size (4).

A second hypothesis is that muscle mass and adipose tissue (MMAT) sequester uremic toxins from extracellular fluid and thus, act as a buffer by diminishing the concentration of toxins in the extracellular fluid. During dialysis treatment (dialytic interval), all of the uremic toxins in the extracellular fluid are rapidly removed. In the time period between dialysis treatments (interdialytic interval), toxins which were sequestered in the MMAT are gradually metered back into the extracellular fluid. The rate at which these toxins are released is determined by two factors: (1) the muscle mass and adipose tissue intercompartmental mass-transfer coefficient (K_{MMAT}); and (2) the difference between the solute concentration in the extracellular fluid and the solute concentration in the muscle mass and adipose tissue (concentration gradient, i.e. C_{MMAT}-C_E). We hypothesize that certain values of the MMAT mass-transfer coefficient (K_{MMAT}) could cause time average solute (toxin) concentrations to be higher in small patients in comparison to large patients.

Although a large patient produces more uremic toxins than a small patient, the large patient has a substantially

© Wichtig Editore, 2007

0391-3988/001-08 $15.00/0

bigger reservoir of MMAT with which to dilute the concentration of these toxins (5). Thus, the MMAT concentration of toxins (C_{MMAT}) for a large patient may be lower than the MMAT concentration of toxin for a small patient. The rate of solute released from the MMAT is directly proportional to the concentration gradient (C_{MMAT}-C_E) between the MMAT and the extracellular fluid. Since the extracellular fluid concentration (C_E) at the beginning of the interdialytic interval is approximately zero, then a lower muscle mass concentration (C_{MMAT}), such as exists in large patients, should result in a lower concentration gradient than in small patients. The lower concentration gradient should lead to a slower release rate of solutes into the extracellular fluid for larger patients. Small patients have a higher MMAT concentration (C_{MMAT}), because they have less muscle mass and adipose tissue with which to dilute the solutes. Thus, small patients should have a high concentration gradient and consequently, a rapid solute release rate. The study by Beddhu et al (5) on body composition and survival in maintenance hemodialysis corroborates this hypothesis. The study shows that patients with a large amount of muscle mass have a lower mortality risk than those with a small amount of muscle mass (5).

In addition, large patients have a larger extracellular fluid compartment with which to further dilute these solutes. The same amount of solute released into both a large and a small patient's extracellular fluid would result in the small patient having a higher concentration than the large patient, because the small patient has a lesser amount of extracellular fluid with which to dilute the solutes.

In summary, the observed higher mortality in small patients may be due to (i) a higher toxin generation rate relative to body mass because of a proportionally larger visceral compartment or (ii) a complex interplay of intercompartmental mass transfer rates and compartmental volumes. A set of three first-order differential Equations [1, 2 and 3] were developed to quantitatively compare and contrast these two hypotheses with a three-pool kinetic model. Equation 1 describes the rate at which toxins are generated in the organ mass (OM) by the high metabolic rate compartment and then released into the extracellular fluid (E). Equation 2 describes the rate at which toxins are released from the muscle mass and adipose tissue (MMAT) into the extracellular fluid (E). Equation 3 describes the rate at which the concentration of toxins in the extracellular fluid varies in accordance with the rate of toxin generation, toxin release from the MMAT and toxin removal by dialysis (K_d).

$$V_{OM}\frac{d(C_{OM})}{dt} = G - K_{OM}(C_{OM} - C_E) \quad [1]$$

$$V_{MMAT}\frac{d(C_{MMAT})}{dt} = K_{MMAT}(C_E - C_{MMAT}) \quad [2]$$

$$V_E\frac{d(C_E)}{dt} = K_{OM}(C_{OM} - C_E) - K_{MMAT}(C_E - C_{MMAT}) - K_d C_E \quad [3]$$

Nomenclature is given in Table I.

METHODS

Refining the governing equations

The explicit solution to the original three Equations [1, 2, and 3], obtained using computational software (Maple 10, Maplesoft, Waterloo, ON, Canada) was impractical due to its complexity and length. To make the solution more manageable, organ mass (OM) was assumed to be at a steady-state, $d(C_{OM})/dt = 0$. This simplifies the system of Equations by making $K_{OM}(C_{OM} - C_E)$ equal to G, and thereby allowing G to be substituted into Equation 3, yielding Equation 5 and obsolescing Equation 1. This substitution results in a pair of Equations for the dialytic interval with manageable solutions [Eq. 4 and 5].

$$V_{MMAT}\frac{d(C_{MMAT})}{dt} = K_{MMAT}(C_E - C_{MMAT}) \quad [4]$$

$$V_E\frac{d(C_E)}{dt} = G - K_{MMAT}(C_E - C_{MMAT}) - K_d C_E \quad [5]$$

To modify the Equations for the interdialytic interval, the dialysis clearance term (K_dC_E) in Equation 5 was eliminated, resulting in Equation 6. However, it was no longer possible to obtain an explicit solution for the pair of Equations [4 and 6] because these Equations can be combined as one Equation with two variables, which is by definition unsolvable. Therefore, an additional Equation 7, which describes the solute mass-balance for the interdialytic interval, was developed. Equation 7 states that toxins generated by the organ mass either enter the extracellular fluid or the MMAT. This additional Equation results in a pair of Equations [6 and 7] for the interdialytic interval with manageable solutions.

$$V_E\frac{d(C_E)}{dt} = G - K_{MMAT}(C_E - C_{MMAT}) \quad [6]$$

$$G = V_E(C_E - C_{E_o}) + V_{MMAT}(C_{MMAT} - C_{MMAT_o}) \quad [7]$$

TABLE I - NOMENCLATURE

BMI	Body Mass Index	Kilograms per Square Meter
BW	Body Weight	Kilograms
C_E	Concentration of Middle Molecule in the Extracellular Fluid	Units of Middle Molecule per Deciliter
C_{Eo}	Initial Concentration of Middle Molecule in the Extracellular Fluid	Units of Middle Molecule per Deciliter
C_{MMAT}	Concentration of Middle Molecule in the Muscle Mass and Adipose Tissue	Units of Middle Molecule per Deciliter
C_{MMATo}	Initial Concentration of Middle Molecule in the Muscle Mass and Adipose Tissue	Units of Middle Molecule per Deciliter
C_{OM}	Concentration in the Organ Mass	Units of Middle Molecule per Deciliter
G	Middle Molecule Generation Rate	Units of Middle Molecule per Minute
HMRC	High Metabolic Rate Compartment	Kilograms
K_d	Dialysis Clearance Rate	Milliliters per Minute
K_{MMAT}	Muscle Mass and Adipose Tissue Mass-Transfer Coefficient	Milliliters per Minute
K_{OM}	Organ Mass Mass-Transfer Coefficient	Milliliters per Minute
PCR	Protein Catabolic Rate	Grams per Day
r	Constant of Integration	Dimensionless
t	Time	Minutes
TAC	Time Average Concentration	Units of Middle Molecule per Deciliter
V_{AT}	Volume of Adipose Tissue	Liters
V_E	Volume of Extracellular Fluid	Liters
V_{MM}	Volume of Muscle Mass	Liters
V_{MMAT}	Volume of Muscle Mass and Adipose Tissue	Liters
V_{OM}	Volume of Organ Mass	Liters

Explicit solution to the revised governing equations

The pair of Equations for the dialytic interval [4 and 5] was solved using computational software (Maple 10, Maplesoft, Waterloo, ON, Canada). Maple 10's algorithm initially decouples the pair of Equations using complex differential algebraic techniques, and then integrates the decoupled Equations to give an explicit solution.

The solution for the interdialytic interval was obtained using the integration method developed by Leibniz. Equations 6 and 7 were consolidated into one Equation by substitution, and then rearranged to isolate the independent variable (C_E). The result is a first-order, separable, differential Equation [Eq. 8]. Both sides of the Equation were multiplied by the integrating factor

$$e^{K_{MM}\left(\frac{1}{V_E}+\frac{1}{V_{MM}}\right)}$$

and then integrated.

$$\frac{d(C_E)}{dt}+K_{MMAT}C_E\left(\frac{1}{V_E}+\frac{1}{V_{MMAT}}\right)=\frac{G}{V_E}\left(1+\frac{K_{MMAT}}{V_{MMAT}}\right)+K_{MMAT}\left(\frac{C_{E_o}}{V_{MMAT}}+\frac{C_{MMAT_o}}{V_E}\right) \quad [8]$$

The constants of integration for the dialytic solution (r_1 and r_2) in Equation 17 were obtained by assuming a boundary condition that the extracellular fluid concentration (C_E) at time zero was equal to the MMAT concentration due to steady-state kinetics. The constant of integration for the interdialytic solution [*r* in Eq. 18] was obtained by assuming the extracellular fluid concentration at time zero is equal to the assumed initial concentration of the extracellular fluid (C_{Eo}).

The time average concentration (TAC) for the interdialytic interval was obtained by numerically integrating the interdialytic solution and then dividing by time. The time interval used was 2.3 days. TAC was calculated for small, medium and large patients with a range of MMAT mass-transfer coefficients: 0.001, 0.01, 0.1, 1 and 5.

Simulations (Table II)

To determine the physical implications of the solutions to the kinetic model, different patient parameters were assumed in order to generate the concentration profiles for the dialytic and interdialytic intervals. Simulations permitted visualizations of the correlation between extracellular solute concentration and time. The simulations consisted of three representative patients: "Small Patient" with a body weight of 40 kg; "Medium Patient" with a body weight of 70 kg; and "Large Patient" with a body weight of 100 kg. Simulations for each patient size were run for a variety of mass transfer coefficients (C_{MMAT}).

The volume of organ mass (V_{OM}) for these representative patients was derived from data and analysis contained in a previous study by Sarkar et al (4), which essentially correlates solute generation to body size. Equation 9 is the result of a linear regression of data from Sarkar et al correlating the percentage of body weight composed of the high metabolic rate compartment ($HMRC_{\%BW}$) and body weight in kilograms (BW) (4). To determine the volume of the HMRC, i.e. organ mass (OM), in terms of body weight, Equation 9 was first multiplied by

TABLE II - PATIENT PARAMETERS

Parameters	BW (kg)	V_E (L)	V_{OM} (L)	V_{MMAT} (L)	G (g/d)	C_{MMATo} (mg/dL)	C_{Eo} (mg/dL)
Basis	Assumed	0.58*BW	BW*(0.33 - 0.0012*BW)	0.0012(BW^2) – 0.01(BW)	1.4(BW) - 0.005(BW2) - 4	Assumed	Assumed
Small Patient	40 kg	23.2 L	11.28 L	1.52 L	44.0 U_{MM} /d	100 U_{MM}/dL	100 U_{MM}/dL
Medium Patient	70 kg	40.6 L	17.22 L	5.18 L	69.5 U_{MM} /d	100 U_{MM}/dL	100 U_{MM}/dL
Large Patient	100 kg	58.0 L	21.00 L	11.00 L	86.0 U_{MM} /d	100 U_{MM}/dL	100 U_{MM}/dL

BW = body weight; V_E = volume of extracellular fluid; V_{OM} = volume of the organ mass; V_{MMAT} = volume of muscle mass and adipose tissue; G = middle molecule generation rate; C_{MMATo} = initial concentration in the muscle mass; C_{Eo} = initial concentration of extracellular fluid.

body weight in kilograms, and then by the average density of the human body (~1 kg/L), resulting in Equation 10. Equation 10 was used to determine the volume of organ mass (V_{OM}) for the three representative patients.

$$HMRC_{\%\ BW} \approx 0.33 - 0.0012\ (BW) \qquad [9]$$

$$HMRC \approx BW*(0.33 - 0.0012\ (BW)) \qquad [10]$$

The generation rate of the middle molecule was derived from the study by Sarkar et al (4), as well. Equation 11 is the result of a linear regression based on data from Sarkar et al correlating protein catabolic rate (PCR) in grams per day and the mass of HMRC in kilograms (4).

$$PCR \approx 4.2\ (HMRC) - 4 \qquad [11]$$

To determine the PCR in terms of body weight, Equation 10 was substituted into Equation 11, resulting in Equation 12. For the purposes of this study, the middle molecule generation rate (G) was considered to be directly proportional to the PCR.

$$G \approx BW*(1.4 - 0.005\ (BW)) - 4 \qquad [12]$$

The volume of the extracellular compartment (V_E) was set at the total body water minus the intracellular fluid. This equals approximately 0.2 times body weight (7).

The volume of muscle mass (V_{MM}) was based on data from Sarkar et al, who studied the correlation between muscle mass volume and total body water (TBW) expressed in Equation 13. Total body water was set at 0.58 times body weight.

$$V_{MM} \approx (0.76*TBW) - 6.80 \qquad [13]$$

This study is only concerned with the part of the muscle mass involved in buffering the solute, i.e. the fluid portion. Thus, Equation 13 was multiplied by the muscle mass's hydration coefficient (0.75), i.e. the relative fraction of water per unit of tissue, resulting in Equation 14 (7). Equation 14 represents the buffering portion of muscle mass correlated with body weight.

$$V_{MM} \approx (0.33*BW) - 5.10 \qquad [14]$$

The volume of adipose tissue (V_{AT}) was derived from data from Sarkar et al (4). The correlation between adipose tissue and body mass index (BMI) is expressed in Equation 15. BMI was converted into body mass by assuming a height of 1.6 m for the representative patients.

$$V_{AT} \approx (1.89*BMI) - 29.20 \qquad [15]$$

The hydration coefficient of adipose tissue is approximately 0.1, meaning that only 10% of the volume of adipose tissue is fluid which is involved in buffering the solute (7). Thus, Equation 15 was multiplied by 0.1, resulting in Equation 16.

$$V_{AT} \approx (0.19*BMI) - 2.92 \qquad [16]$$

Equations 14 and 16 were summed to give the volume of muscle mass and adipose tissue involved in buffering the solute.

The initial extracellular and MMAT concentrations were assumed to be equal due to steady-state kinetics and set at 10 U_{MM}/dL for the simulations, where U is an arbitrary number of units of concentration of the hypothetical intermediate molecular weight species (IMWS). The initial extracellular concentration (C_{Eo}) for the interdialytic interval is the extracellular concentration at the end of the dialytic interval simulation. The length of the dialytic interval was set at 4 hours with a dialysis clearance rate (K_d) of 200 ml/min.

RESULTS

Explicit analytical solutions to the modeled equations

The explicit solution for the pair of Equations modeling the dialytic interval (Eq. 4 and 5) is the set of Equations 17, where r_1 and r_2 are constants of integration. This set describes how the concentration in the extracellular fluid varies over time.

$$C_E = r_1\xi_1 e^{\lambda_1 t} + r_2\xi_2 e^{\lambda_2 t} + \frac{G}{K_d} \quad [17]$$

$$\lambda_1 = -\frac{1}{2V_E V_{MMAT}}\left(V_{MMAT}K_d + V_E K_{MMAT} + K_{MMAT}V_{MMAT} - \sqrt{\left(V_{MMAT}K_d + V_E K_{MMAT} + K_{MMAT}V_{MMAT}\right)^2 - 4K_{MMAT}V_{MMAT}K_d V_E}\right)$$

$$\lambda_2 = -\frac{1}{2V_E V_{MMAT}}\left(V_{MMAT}K_d + V_E K_{MMAT} + K_{MMAT}V_{MMAT} + \sqrt{\left(V_{MMAT}K_d + V_E K_{MMAT} + K_{MMAT}V_{MMAT}\right)^2 - 4K_{MMAT}V_{MMAT}K_d V_E}\right)$$

$$\xi_1 = \frac{1}{2} - \frac{1}{2V_E}\left(\frac{V_{MMAT}K_d}{K_{MMAT}} + V_{MMAT} + \frac{1}{K_{MMAT}} \cdot \sqrt{\left(V_{MMAT}K_d + V_E K_{MMAT} + K_{MMAT}V_{MMAT}\right)^2 - 4K_{MMAT}V_{MMAT}K_d V_E}\right)$$

$$\xi_2 = \frac{1}{2} - \frac{1}{2V_E}\left(\frac{V_{MMAT}K_d}{K_{MMAT}} + V_{MMAT} - \frac{1}{K_{MMAT}} \cdot \sqrt{\left(V_{MMAT}K_d + V_E K_{MMAT} + K_{MMAT}V_{MMAT}\right)^2 - 4K_{MMAT}V_{MMAT}K_d V_E}\right)$$

Equation 18 is the explicit solution for the pair of equations modeling the interdialytic interval [Eq. 6 and 7], where *r* is the constant of integration. This equation states the extracellular fluid concentration as a function of time.

$$C_E = \frac{G(V_{MMAT} + K_{MMAT}) + K_{MMAT}(C_{E_o}V_E + C_{MMAT_o}V_{MMAT})}{K_{MMAT}(V_{MMAT} + V_E)} + re^{-K_{MMAT}\left(\frac{1}{V_E} + \frac{1}{V_{MMAT}}\right)t} \quad [18]$$

Simulations based on the analytic solutions

Figure 1 displays concentration vs. time during dialysis for the three representative patients with the parameters given in Table II and a MMAT mass-transfer coefficient (K_{MMAT}) of 0.1 ml/min. Simulations for a large range of MMAT mass-transfer coefficients (100 ml/min to 0.0001 mL/min) yielded virtually identical results.

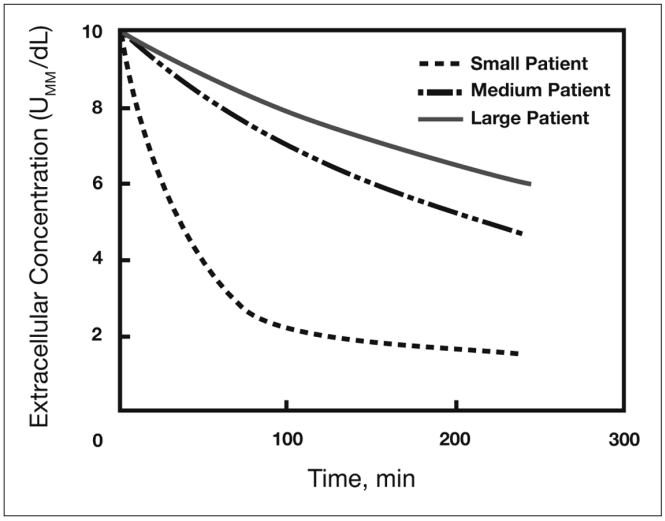

Fig. 1 - *Predicted IMWS solute concentration during dialysis. Plot of the concentration of a hypothetical middle molecule in the extracellular fluid versus time during the dialytic interval with the muscle mass and adipose tissue mass-transfer coefficient set to 0.1 ml/min and the dialysis clearance rate equal to 200 ml/min. Lines are for three different hypothetical patients defined in Table I; starting concentration for the hypothetical middle molecule is set at 10 U_{MM}/dL; and the length of treatment is set at 4 hours for each patient. The graph shows that the small patient has a lower final concentration than the other patients and that the small patient reaches its final steady-state concentration within 4 hours, while the medium and large patients do not, as would be expected. Results are virtually identical for a wide range of MMATs.*

Figure 2 displays the interdialytic solution graphed for the three hypothetical patients with the parameters given in Table I and for four different values of the MMAT mass-transfer coefficient (K_{MMAT} = 5, 0.1, 0.01, and 0.001).

Figure 3 charts the time average concentration as the MMAT mass-transfer coefficient varies between 5 and 0.001 for the interdialytic interval for the three representative patients with the parameters given in Table II. The time interval used was 2.3 days.

DISCUSSION

This study's focus was to determine if kinetic modeling could provide an explanation of why smaller patients have a relatively higher mortality risk than larger patients on maintenance hemodialysis. A three-pool urea-kinetic model was developed to mathematically represent an explanation. The model was modified to yield a more manageable solution, and then solved using computational software. Simulations were performed for a set of three

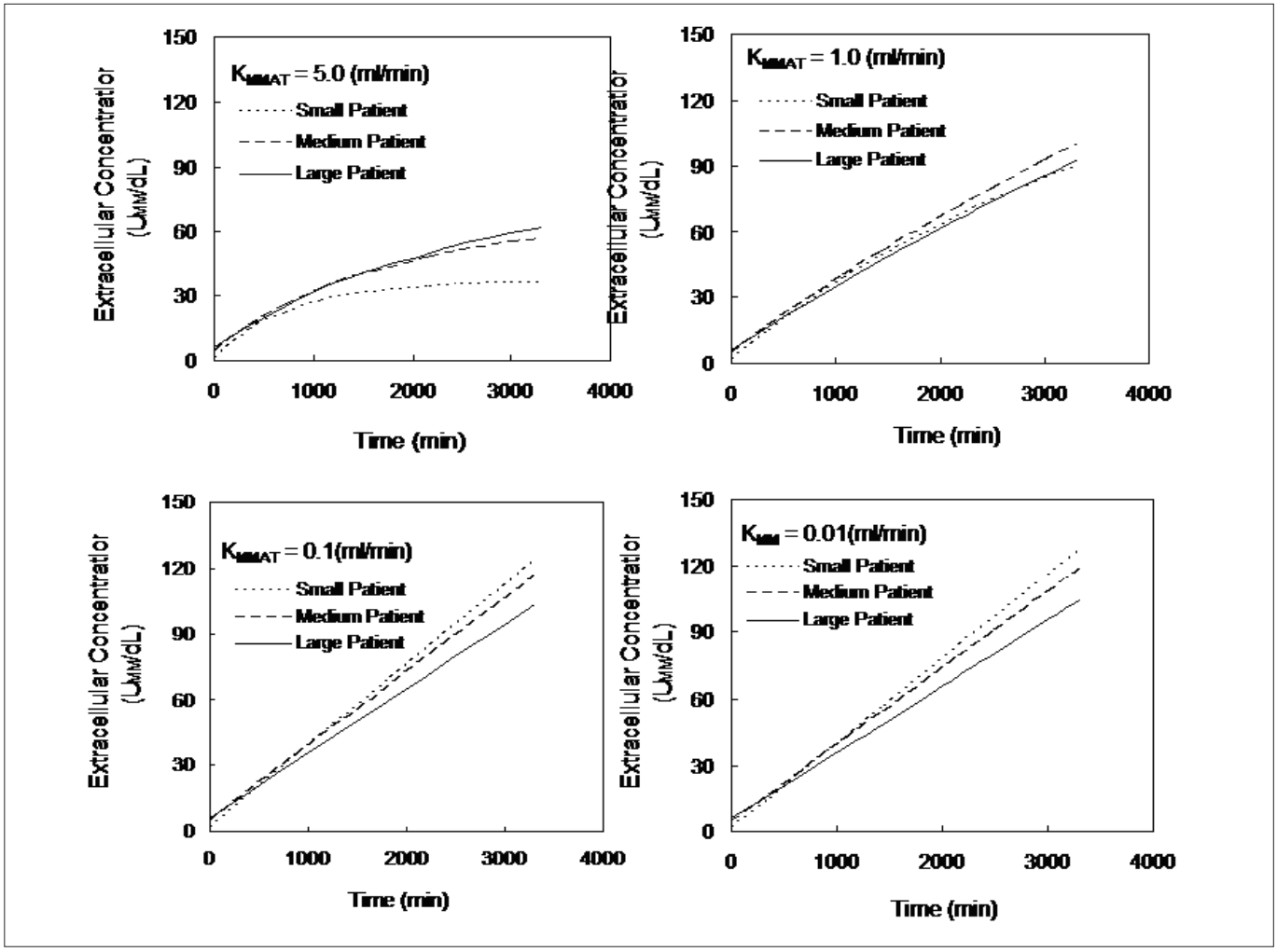

Fig. 2 - *Predicted IMWS solute concentration during the interdialytic. Plots of extracellular fluid concentration of a hypothetical middle molecule versus time during the interdialytic interval with MMAT mass-transfer coefficient varied from 5 ml/min to 0.01 ml/min. Lines are for three different hypothetical patients defined in Table II; and the starting extracellular fluid concentration of the hypothetical middle molecule is set at the corresponding final concentration following dialysis. The graph with K_{MMAT} equaling 5 ml/min shows the small patient reaches its steady-state concentration before the other patients. Also, the small patient's steady-state concentration is lower than that of the larger patients. However, the other remaining plots indicate that as K_{MMAT} decreases both the final steady-state concentration and the time required to reach the steady-state concentration increase. Thus, small patients will be particularly vulnerable to middle molecules which exchange slowly between fat-muscle and extracellular fluid.*

representative patients of different body weights, resulting in rates at which solutes move into and out of the muscle mass and adipose tissue (MMAT).

Figure 1 demonstrates that small patients have a lower extracellular concentration than medium or large patients at the end of a hemodialysis treatment session. These results are independent of the MMAT mass-transfer coefficient because a large range of values for the MMAT mass-transfer coefficient yielded similar results. These results are consistent with expectations in that transfer between extracellular fluid and MMAT is too slow to have any significant impact on the dialysis kinetics. However, this is not true for the interdialytic interval.

Analysis of the solution for the interdialytic interval (Fig. 2) implies several physiological differences between large patients and small patients on maintenance hemodialysis. First, for solutes with a low value of K_{MMAT}, small patients exhibit a higher extracellular fluid concentration of the hypothetical middle molecule than their larger counterparts. In Figure 2, the graph with a MMAT mass-trans-

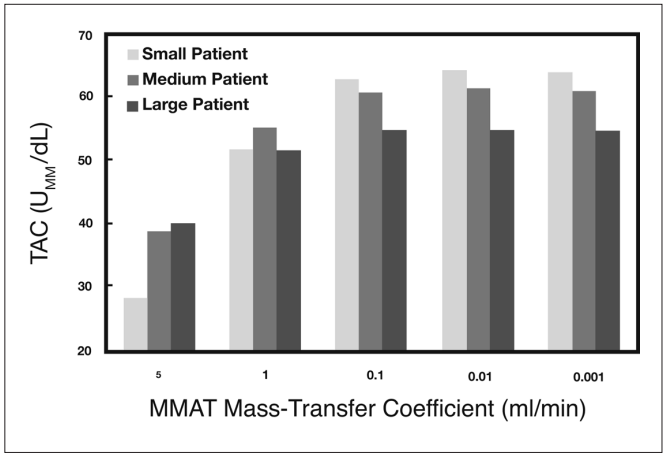

Fig. 3 - *Predicted TAC of IMWS solute during interdialytic interval. Chart of the time average (TAC) during the interdialytic interval for hypothetical middle molecules with a range of values for the muscle mass and adipose tissue (MMAT) mass-transfer coefficient during the interdialytic interval. Each set of bars is composed of three hypothetical patients with selected parameters given in Table I. The chart identifies the values of MMAT for under which TAC would be significantly lower in patients with a higher volume of muscle mass and adipose tissue.*

fer coefficient of 5 ml/min shows that the small patient's steady-state concentration is approximately 30 U_{MM}/dL. Note that the large and medium patients have yet to reach a steady-state concentration within the timeframe, but that the concentration value is asymptoting toward a higher value than that of the small patient's. The high metabolic rate compartment hypothesis predicts this effect since large patients have a larger high metabolic rate compartment, and thus, a higher generation rate of toxins in comparison with a small patient (4).

Second, small patients, initially, have a higher rate of extracellular concentration increase than larger patients. Figure 2 demonstrates that the small patient's extracellular fluid concentration increases faster than that of the large patient, except at high K_{MMAT} values. This result is consistent with predictions by the muscle mass and adipose tissue hypothesis. Small patients have a faster release rate because they initially have a larger concentration gradient (C_{MMAT} - C_E) due to their relatively high MMAT concentration. Once these solutes are released into the extracellular fluid, small patients have a smaller extracellular fluid volume with which to dilute these solutes than large or medium patients, further increasing their extracellular fluid concentration. Both of these factors cause the extracellular fluid concentration in small patients to increase more rapidly than in large or medium patients. Figure 2 further shows that for low values of the MMAT mass-transfer coefficient, small patients have a higher extracellular fluid concentration at the end of the interdialytic interval than both the medium and large patients.

Third, as the value of the MMAT mass-transfer coefficient (K_{MMAT}) decreases, the time-average concentration (TAC) of IMWS solutes for all body weights increases, and the difference between the TAC of a small and large patient increases. Figure 3 exhibits the relationship between TAC in the extracellular fluid and the MMAT mass-transfer coefficient during the interdialytic interval. As shown, TAC increases as the MMAT mass-transfer coefficient decreases for all body weights. However, TAC increases less rapidly for large patients than for small ones. Thus, the difference between the TAC of a large patient and the TAC of a small patient is inversely correlated with the value of the MMAT mass-transfer coefficient. Thus, small patients are especially vulnerable to uremic toxins which exchange slowly between muscle-mass/adipose tissue and the extracellular fluid.

The hypothesized explanations for the discrepancy of mortality risk among patients with different body weights contribute to the paradoxical relationship of relative mortality and body weight for maintenance hemodialysis patients. On one hand, a higher ratio of visceral mass (V_{OM}) to extracellular fluid volume (V_E) in small patients necessarily leads to a higher time-average toxin concentration. But this may not be the whole story. Toxic middle molecules, which are slowly exchanged between muscle mass and adipose tissue, i.e. V_{MM} and V_{AT}, have been predicted to have a higher time-average concentration in small patients when compared to large patients. This could represent a further risk factor for patients in the small BMI cohort.

Address for correspondence:
Drew Cronin-Fine
166 Elizabeth Street Apt. #B
New York
New York 10012 - USA
e-mail: DCronin-Fine@imshealth.com

REFERENCES

1. Port FK, Ashby VB, Dhingra RK, Roys EC, Wolfe RA. Dialysis Dose and Body Mass Index Are Strongly Associated with Survival in Hemodialysis Patients. J Am Soc Nephrol 2002; 13: 1061-6.
2. Wolfe RA, Ashby VB, Daugirdas JT, Agodoa LY, Jones CA, Port FK. Body Size, Dose of Hemodialysis, and Mortality. Am J Kidney Dis 2000; 35: 80-8.
3. Conway B, Rene A. Obesity as a disease: no lightweight matter. Obes Rev 2004; 5: 145-51.
4. Sarkar SR, Kuhlmann MK, Kotanko P, Zhu F, Heymsfield SB, Wang J, Meisels IS, Gotch FA, Kaysen GA, Levin NW. Metabolic Consequences of Body Size and Body Composition in Hemodialysis Patients. (Submitted for publication).
5. Beddhu S, Pappas LM, Ramkumar N, Samore M. Effects of Body Size and Body Composition on Survival in Hemodialysis Patients. J Am Soc Nephrol 2003; 14: 2366-72.
6. Agar JW, Mahadevan K, Knight R, Antonis ML, Somerville CA. “Flexible” or “lifestyle” dialysis: Is this the way forward? Nephrology 2005; 10: 525-9.
7. Boer P. Estimated lean body mass as an index for normalization of body fluid volumes in humans. Am J Physiol 1984; 247: F632-6.